Monte Carlo Simulation of Phase Equilibria of Aqueous Systems

Ioannis G. Economou

Molecular Modelling of Materials Laboratory

Institute of Physical Chemistry

National Research Center for Physical Sciences Demokritos

GR-15310 Aghia Paraskevi Attikis, Greece

e-mail: economou@mistras.chem.demokritos.gr

For presentation at the 14th Symposium on Thermophysical Properties

Boulder, Colorado, USA, June 25-30, 2000

Keywords: molecular simulation, vapour-liquid equilibria, aqueous mixtures, molecular models, Expanded Ensemble.

Abstract

In this article, an overview of recent achievements in Monte Carlo molecular simulation of aqueous systems is presented. Semi-empirical two-body potential models introduced recently allow accurate representation of the pure water vapor-liquid equilibria, including the critical region. Furthermore, these models are used for the calculation of water - hydrocarbon low and high pressure phase equilibria. Efficient methodologies for the simulation of highly dense systems and / or systems of long chain molecules are discussed. In all cases, simulation results are compared against experimental data. Limitations of approximate molecular models are discussed.

Introduction

The thermodynamic properties and phase behavior of aqueous systems are of great interest for biological and technological processes. The accurate knowledge of these properties is vital for the optimum design of chemical and environmental engineering processes. Although an impressive amount of data are available in the literature for different aqueous systems over a wide range of conditions (temperature, pressure and composition), predictive models are always necessary given the considerable cost and time of the experimental work as well as the fact that it is impossible to examine experimentally all of the different systems and conditions involved in a given process.

Molecular simulation has advanced to a point where it can be used for accurate complex fluid property calculations [1-2]. Furthermore, it provides the unique advantage of allowing elucidation of microscopic mechanisms that affect macroscopic behavior. In order that simulation results are directly comparable to experimental data, realistic molecular models that capture accurately intramolecular and intermolecular interactions are necessary. In this respect, a large number of molecular models have been proposed for water [3-15]. These models are divided into those accounting explicitly for two-body interactions only [3-8, 13-14] and those that calculate explicitly many body effects (such as polarizability) as well [9-12, 15]. The former type of models account for the many body effects implicitly through the tuning of model parameters using liquid state properties and are considerably faster (by a factor of 10 approximately) compared to the many-body potentials [9, 14]. Furthermore, many-body potentials have not proven more accurate for phase equilibrium calculations, yet [15, 16]. This is mainly due to considerable computing time needed to tune these more complex models. As a result, semi-empirical two-body models have gained

considerable popularity for phase equilibrium calculations and are used for all calculations presented here.

Efficient Monte Carlo simulation methodologies are required for highly dense fluids such as the aqueous systems. An impressive number of highly innovative schemes were proposed in the last decade. The Gibbs Ensemble Monte Carlo (GEMC) method was the first, and still very popular, scheme allowing efficient simultaneous simulation of two phases in equilibrium [17]. More recent methodologies include the Gibbs-Duhem integration method [18], the histogram reweighting Grand Canonical Monte Carlo [19] method, and the development of pseudo-ensembles [20, 21].

A key property in phase equilibrium is the chemical potential of the different species in the phases examined. The Widom approach used widely for pure components and mixtures relies on random insertions of 'ghost' molecules into the system simulated and calculation of the interaction energy of the 'ghost' molecule with the remaining molecules of the system [22]. This method becomes progressively impractical for highly dense systems and/or when the size of the inserted molecule(s) increases. Alternative more efficient methodologies based on particle deletion [23-24], chain increment Ansatz [25] and expanded ensemble have been proposed [26-28]. Calculations with some of these other methods are presented here.

In the following sections, a brief presentation of several potential models for water is made, followed by a discussion of simulation methodologies for phase equilibria. Finally, simulation results are presented for pure water and water – hydrocarbon mixtures. In all cases, comparisons are made against experimental data.

Potential Models

Two-body molecular models are used in this work for water. In all cases, water is modelled as a three-site model, that is an oxygen site (exhibiting non-polar and electrostatic interactions) and two hydrogen sites (exhibiting electrostatic interactions, only). The relative positions of these three sites on the water molecule are assumed constant for all models. Two different representations are used for the non-polar interactions: In SPC [7], SPC/E [8] and MSPC/E [13] the Lennard-Jones potential is used whereas in the Errington and Paragiotopoulos model [14], the Buckingham exponential-6 (exp-6, in short) model is assumed. As a result, for the SPC, SPC/E and MSPC/E model, the interaction energy between two water molecules is given from the expression:

$$u(r)=4\varepsilon\left[\left(\frac{\sigma}{r}\right)^{12}-\left(\frac{\sigma}{r}\right)^{6}\right]+\sum_{\gamma=1}^{3}\sum_{\delta=1}^{3}\frac{1}{4\pi\varepsilon_0}\frac{q_\gamma q_\delta}{r_{\gamma\delta}} \qquad (1)$$

whereas for the exp-6 model, it is:

$$u(r)=\begin{cases}\dfrac{\varepsilon}{1-6/\alpha}\left[\dfrac{6}{\alpha}\exp\left(\alpha\left[1-\dfrac{r}{r_m}\right]\right)-\left(\dfrac{r_m}{r}\right)^{6}\right]+\displaystyle\sum_{\gamma=1}^{3}\sum_{\delta=1}^{3}\frac{1}{4\pi\varepsilon_0}\frac{q_\gamma q_\delta}{r_{\gamma\delta}} & for\ r > r_{\max} \\ \infty & for\ r < r_{\max}\end{cases} \qquad (2)$$

Parameter values for the different models are given elsewhere [13,14]. For the MSPC/E and exp-6 model, the parameters were optimized in order to reproduce best the experimental vapor – liquid equilibrium of pure water. In all cases, long-range electrostatic interactions are calculated using the Ewald summation technique [13, 14].

Hydrocarbon molecules are modeled using a united atom representation (hydrogen atoms are not accounted explicitly). Bond lengths are kept constant whereas for the higher hydrocarbons examined here, bond bending angles and torsional angles are variable. Non-bonded intramolecular and intermolecular interactions are calculated

using a Lennard-Jones potential, the so-called TraPPE potential [29], and an exp-6 potential, in the spirit presented above for water. Details on these potentials together with parameter values optimized for phase equilibrium properties can be found in refs. [27–30]. Non-polar interactions between unlike groups are calculated using the Lorentz-Berthelot combining rules.

Simulation Methodologies

Pure water vapor-liquid equilibrium was simulated using the GEMC-NVT method that consists of random particle displacement, volume fluctuation and particle interchange between the two simulation boxes. The average pressure was calculated explicitly in the course of the simulation using an equation based on the molecular virial expression [13]. The size of the system studied was in the order of 200 – 250 molecules. Water – methane and water – ethane mixtures at high pressure were examined using GEMC-NPT simulation. In this case, a typical simulation consisted of approximately 200 water molecules and 100 hydrocarbon molecules [30].

An efficient pure component phase equilibrium methodology was developed by Errington and Panagiotopoulos [31] using Hamiltonian Scaling Grand Canonical histogram reweighting Monte Carlo (HSGCMC) that allows simultaneous sampling of multiple Hamiltonians and / or state points. In this way, one is able to test several Hamiltonians within reasonable CPU time.

Small hydrocarbon solubilities in water are usually expressed in terms of Henry's law constant, $H_{hc\to w}$, [32]. Using standard thermodynamic relations, the Henry's law constant can be expressed in terms of the hydrocarbon excess chemical potential in water:

$$H_{hc\to w} = \lim_{x_{hc}\to 0}\left(\frac{\rho_w}{\beta}\exp\left(\beta\mu_{hc}^{ex}\right)\right) \qquad (3)$$

where ρ_w is the pure water number density and $\beta = 1/k_BT$. Calculation of μ_{hc}^{ex} is usually performed by using the Widom test particle insertion method [22]. According to this method, a solute particle is inserted in the well equilibrated solvent and μ_{hc}^{ex} is evaluated from the total energy on the test molecule by the water molecules on the system. This method is used here for the case of methane and of ethane dissolved in water.

Widom insertion method becomes impractical for dense solvents and / or large solute molecules. An alternative methodology is to remove a test particle from the system (going from an *N*-molecule system to an (*N-1*)-molecule system) and calculate the corresponding energy change [24]. The particle removal is done in two stages using an intermediate system that consists of an (*N-1*)-molecule and one hard core molecule. Accordingly, μ^{ex} is calculated from the expression:

$$\beta\mu^{ex} = -\ln\left(\left\langle\frac{1}{V}\right\rangle\frac{Z(N,P,T)}{Z(N-1,P,T)}\right) = -\ln\left(\left\langle\frac{1}{V}\right\rangle\frac{\left\langle\prod_{i=1}^{N-1}H\left(r_{i,N}\right)\right\rangle_{N-1,P,T}}{\left\langle\prod_{i=1}^{N-1}H\left(r_{i,N}\right)\frac{\exp\left(\beta U^{(N)}\left(\vec{r}_1,\ldots,\vec{r}_N\right)\right)}{V}\right\rangle_{N,P,T}}\right) \qquad (4)$$

where $H(r_{i,N})$ is a Heaviside step function and $U^{(N)}\left(\vec{r}_1,\ldots,\vec{r}_N\right)$ is the intermolecular energy felt by the *N*th molecule due to its interactions with the remaining *N-1* molecules of the system. This approach reduces the CPU time required compared to the Widom method by up to an order of magnitude, depending on the conditions [24].

Another efficient method to calculate excess chemical potential of large molecules is based on the combination of Widom insertion and Expanded Ensemble [26-28]. A scaling parameter γ $\hat{\mathbf{I}}$ *[0,1]* is used to scale the full Hamiltonian of the solute molecule

(parameters ε and σ for a Lennard-Jones potential and parameters ε, σ and α for an exp-6 potential, respectively). Initially, μ^{ex} of the "weak" molecule is calculated using Widom insertions. Followed this initial calculation, a number of sub-ensembles are sampled. Each of these sub-ensembles consists of *N* solvent (water) molecules and one solute (hydrocarbon) molecule with a different γ value (different Hamiltonian). In the course of the simulation, attempts are made to move from one sub-ensemble to another. Each Hamiltonian should be sampled with equal frequency and so weighting functions are introduced. The difference in μ^{ex} of two Hamiltonians, i.e. *i* and *j,* is evaluated by the expression:

$$\beta\mu^{ex}(\gamma_j) - \beta\mu^{ex}(\gamma_i) = -\ln\left(\frac{p_j}{p_i}\right) + \ln\left(\frac{\omega_j}{\omega_i}\right) \qquad (5)$$

where p_i is the probability of visiting sub-ensemble *i* and ω_i is the weight of Hamiltonian *i*. The total μ^{ex} is the sum of the differences between adjacent sub-ensembles and of μ^{ex} of the "weak" molecule from the Widom insertions.

Results and Discussion

Pure component. Pure water saturated density and vapor pressure simulation results from SPC, SPC/E, MSPC/E and exp-6 together with experimental data are shown in Figures 1 and 2, respectively. SPC and SPC/E molecular models were developed to represent accurately water properties at ambient conditions and so they become progressively inaccurate as temperature increases. MSPC/E is essentially a re-parameterization of the SPC/E model using simple scaling arguments with the aim to reproduce accurately the phase equilibrium of pure water with emphasis to the vapor pressure which controls mixture phase equilibria [13]. Parameterization of the exp-6

model focused on the accurate representation of the coexistence curve, vapor pressure and critical properties of pure water [14]. In the temperature range 300 – 600 K, the average deviation between experimental and simulation data for the vapor pressure is 10 % from the MSPC/E and the exp-6 model (with the exp-6 being more accurate at lower temperatures and MSPC/E more accurate at higher temperatures), and 40 % from the SPC/E model, respectively. Exp-6 reproduces accurately the saturated liquid density with an average deviation of 3 % whereas SPC/E and MSPC/E are slightly less accurate with an average deviation in the order of 5 % for each model.

In Table 1, the critical parameters for pure water from each model are compared to the experimental data. Exp-6 critical temperature essentially coincides with the experimental value. On the other hand, all models predict a lower critical pressure compared to the experimental value. For comparison, the critical temperature values from several polarizable water models reported in the literature are in the range 495 – 685 K [15-16]. The microscopic structure of water has been also calculated using most of these models [8, 10, 12-15].

Aqueous mixtures. The Henry's law constant of methane in water at saturated conditions is shown in Figure 3. Simulation results from the Widom test particle insertion method using the SPC/E and MSPC/E models for water and TraPPE model for methane [29] are in good agreement with the experimental data, although MSPC/E is closer to the experimental data up to 450 K. This is an indication that a more accurate model for the pure water results also in better mixture predictions. Similarly accurate simulation results were obtained for the Henry's constant of ethane in water [30]. Preliminary calculations using the test particle deletion scheme [24] at 300 K resulted in lower statistical uncertainty and lower CPU time compared to the results from the Widom insertion method. Recent results from molecular dynamics simulations for μ^{ex}

of methane and of ethane at 298 K using the SPC model are in good agreement with the results presented here [32].

High pressure phase equilibria for water – methane mixture at 423 K, 523 K and 603 K are shown in Figure 4 using MSPC/E-TraPPE and exp-6 models, respectively. Simulation results from both sets of models are in good agreement with the experimental data over the entire pressure range. In Figure 5, the high pressure phase equilibria of water – ethane mixture at 523 K, 573 K and 623 K are shown. Simulation results from the exp-6 capture qualitatively the phase behavior of the mixture. In all cases however, simulation predicts lower water solubility in ethane than experimentally measured. At 623 K, a narrow window of complete miscibility is observed in the pressure range 680 – 760 bar. Simulation in the pressure range 500 – 1000 bar indicated that the model predicts complete miscibility. This is a direct evidence that accurate molecular models are able to predict complex phase behavior.

The Henry's law constant of n-butane and of n-hexane in water was calculated using the Widom insertion with Expanded Ensemble methodology. In Figure 6, simulation results from the exp-6 model are compared against experimental data. The model captures qualitatively the experimental behavior: For the higher hydrocarbon, the Henry's law constant is higher at a given temperature. Furthermore, a maximum value for Henry's constant is predicted at approximately 370 K in agreement with the experimental data. However, in both cases simulation predicts lower Henry's constant values and thus higher solubilities. A different set of combining rules did not result in a substantial improvement [28]. In Figure 7, experimental data [33] and simulation calculations from the exp-6 model [27] are shown for the Henry's constant of cyclohexane and of benzene in water. Qualitative agreement is observed. However, the model predicts higher solubility for cyclohexane and lower solubility for benzene

compared to the experimental data. These deviations should be attributed to the approximate nature of the molecular potentials that become substantially inaccurate for highly non-ideal asymmetric mixtures.

Conclusions

Significant advances have been made recently in the development of novel methodologies for the efficient molecular simulation of highly non-ideal mixture phase equilibria. In this way, it is possible to obtain quantitative results for systems at remote conditions, as for example at very high pressure. Based on the results presented here and elsewhere, it is apparent that more complex potentials that account explicitly for polarizability and other many body effects are necessary.

References

[1] M.W. Deem, AIChE J., 44 (1998) 2569.

[2] A.Z. Panagiotopoulos, J.Phys: Condens. Matter, 12 (2000) R25.

[3] J.D. Bernal and R.H. Fowler, J. Chem. Phys., 1 (1933), 515.

[4] F.H. Stillinger and A. Rahman, J. Chem. Phys., 60 (1974), 1545.

[5] W.L. Jorgensen, J. Chem. Phys., 77 (1982), 4156.

[6] W.L. Jorgensen, J. Chandrasekhar, J.D. Madura, R.W. Impley, M.L. Klein, J. Chem. Phys., 79 (1983), 926.

[7] H.J.C. Berendsen, J.P.M. Postma, W.F. van Gunsteren and J. Hermans, in B. Pullman (Ed.), Intermolecular Forces, Reidel, Dordrecht, 1981.

[8] H.J.C. Berendsen, J.R. Grigera and T.P. Straatsma, J. Phys. Chem., 91 (1987), 6269.

[9] P. Ahlstrom, A. Wallqvist, S. Engström and B. Jönsson, Mol. Phys., 68 (1989), 563.

[10] J. Caldwell, L.X. Dang and P.A. Kollman, J. Am. Chem. Soc., 112 (1990), 9144.

[11] A. Wallqvist, B.J. Berne, J. Chem. Phys., 97 (1993), 13841.

[12] A.A. Chialvo and P.T. Cummings, J. Chem. Phys., 105 (1996), 8274.

[13] G.C. Boulougouris, I.G. Economou and D.N. Theodorou, J. Phys. Chem. B, 102 (1998), 1029.

[14] J.R. Errington and A.Z. Panagiotopoulos, J. Phys. Chem. B, 102 (1998), 7470.

[15] A.D. Mackie, J. Hernández-Cobos and L.F. Vega, J. Chem. Phys., 111 (1999), 2103.

[16] K. Kiyohara, K.E. Gubbins and A.Z. Panagiotopoulos, Mol. Phys., 94 (1998), 803.

[17] A.Z. Panagiotopoulos, Mol. Phys., 61 (1987), 813.

[18] D.A. Kofke, J. Chem. Phys., 98 (1993), 4149.

[19] N.B. Wilding, Phys. Rev. E, 52 (1995), 602.

[20] D. Spyriouni, I.G. Economou and D.N. Theodorou, Phys. Rev. Lett., 80 (1998), 4466.

[21] F.A. Escobedo, J. Chem. Phys., 108 (1998), 8761.

[22] B. Widom, J. Chem. Phys., 39 (1963), 2808.

[23] D.A. Kofke and P.T. Cummings, Mol. Phys., 92 (1997), 973.

[24] G.C. Boulougouris, I.G. Economou and D.N. Theodorou, Mol. Phys., 96 (1999), 905.

[25] S.K. Kumar, I. Szleifer and A.Z. Panagiotopoulos, Phys. Rev. Lett., 66 (1991), 2935.

[26] A.P. Lyubartsev, A.A. Martsinovski, S.V. Shevkunov, P.N. Vorontsov-Velyaminov, J. Chem. Phys., 96 (1992), 1776; A.P. Lyubartsev, A. Laaksonen, P.N. Vorontsov-Velyaminov, Mol. Simul., 18 (1996), 43; A.P. Lyubartsev, O.K. Førrisdhahl, A. Laaksonen, J. Chem. Phys., 108 (1998), 227.

[27] J.R. Errington and A.Z. Panagiotopoulos, J. Chem. Phys., 111 (1999), 9731.

[28] G.C. Boulougouris, J.R. Errington, I.G. Economou, A.Z. Panagiotopoulos and D.N. Theodorou, J. Phys. Chem. B (2000) in press.

[29] M.G. Martin and J.I. Siepmann, J. Phys. Chem. B., 102 (1998), 2569.

[30] J.R. Errington, G.C. Boulougouris, I.G. Economou, A.Z. Panagiotopoulos and D.N. Theodorou, J. Phys. Chem. B, 102 (1998), 8865.

[31] J.R. Errington and A.Z. Panagiotopoulos, J. Chem. Phys., 109 (1998), 1093.

[32] J.T. Slusher, J. Phys. Chem. B, 103 (1999), 6075.

[33] C. Tsonopoulos and G.M. Wilson, AIChE J., 29 (1983), 990.

[34] J.J. de Pablo, J.M. Prausnitz, H.J. Strauch and P.T. Cummings, J. Chem. Phys., 93 (1990), 7355.

[35] Y. Guissani and B. Guillot, J. Chem. Phys., 98 (1993), 8221.

[36] J. Alejandre, D.J. Tildesley and G.A. Chapela, J. Chem. Phys., 102 (1995), 4574.

[37] NIST Chemistry Webbook, NIST Standard Reference Database Number 69, 2000. http://webbook.nist.gov/chemistry/.

[38] A.H. Harvey, AIChE J., 42 (1996), 1491.

[39] R.G. Sultanov, V.G. Skripka and N.A. Yu, Zh. Fiz. Khim., 46 (1972), 2160.

[40] A. Danneil, K. Toedheide and E.U. Franck, Chemie-Ing. Techn., 39 (1967), 816.

[41] J.J. Carroll, F.-Y. Jou and A.E. Mather, Fluid Phase Equilib., 140 (1997), 157.

Table 1. Critical parameters for pure water.

Model	T_c (K)	P_c (bar)	ρ_c (g/cm^3)	Z_c	Reference
SPC	587	-	0.27	-	[34]
	596	126	0.289	0.158	[13]
	593.8	129	0.271	0.173	[14]
SPC/E	640	160	0.29	0.187	[35]
	630.4	-	0.308	-	[36]
	630	148	0.295	0.172	[13]
	638.6	139	0.273	0.173	[14]
MSPC/E	602	148	0.310	0.172	[13]
	609.8	139	0.287	0.172	[14]
exp-6	645.9	183	0.297	0.207	[14]
Experimental	647.1	220.64	0.322	0.229	[37]

Figure captions

Figure 1. Pure water vapor-liquid equilibria. Experimental data (solid line) [37], and molecular simulation results from SPC (triangles), SPC/E (diamonds), MSPC/E (squares) (all from ref. [13]) and exp-6 (open circles) [14] models. Error bars are omitted for clarity.

Figure 2. Pure water vapor pressure. Symbols are the same as in Figure 1.

Figure 3. Henry's law constant of methane in water. Experimental data (solid line) [38] and Widom insertion Monte Carlo simulations from the SPC/E (diamonds), and MSPC/E (squares) models for water. The TraPPE model [29] was used for methane.

Figure 4. Water – methane phase equilibria. Experimental data [39] at 423 K (solid lines), 523 K (short dashed lines) and 603 K (long dashed lines) and GEMC simulation results [30] from the MSPC/E-TraPPE (solid squares at 423 K and 603 K and open squares at 523 K) and exp-6 (filled circles at 423 K and 603 K and open circles at 523 K) models.

Figure 5. Water – ethane phas equilibra. Experimental data [40] at 523 K (solid lines), 573 K (short dashed lines) and 623 K (long dashed lines) and GEMC simulation results [30] from the exp-6 (circles at 523 K, diamonds at 573 K and triangles at 623 K) model.

Figure 6. Henry's law constant of n-butane and of n-hexane in water. Experimental data [33, 41] (solid line for n-butane and dashed line for n-hexane) and Widom insertion + Expanded Ensemble Monte Carlo simulation (diamonds for n-butane and triangles for n-hexane).

Figure 7. Henry's law constant of cyclohexane and of benzene in water. Experimental data [33] (dashed line for cyclohexane and solid line for benzene) and Widom insertion + Expanded Ensemble Monte Carlo simulation (triangles for cyclohexane and diamonds for benzene) [27].

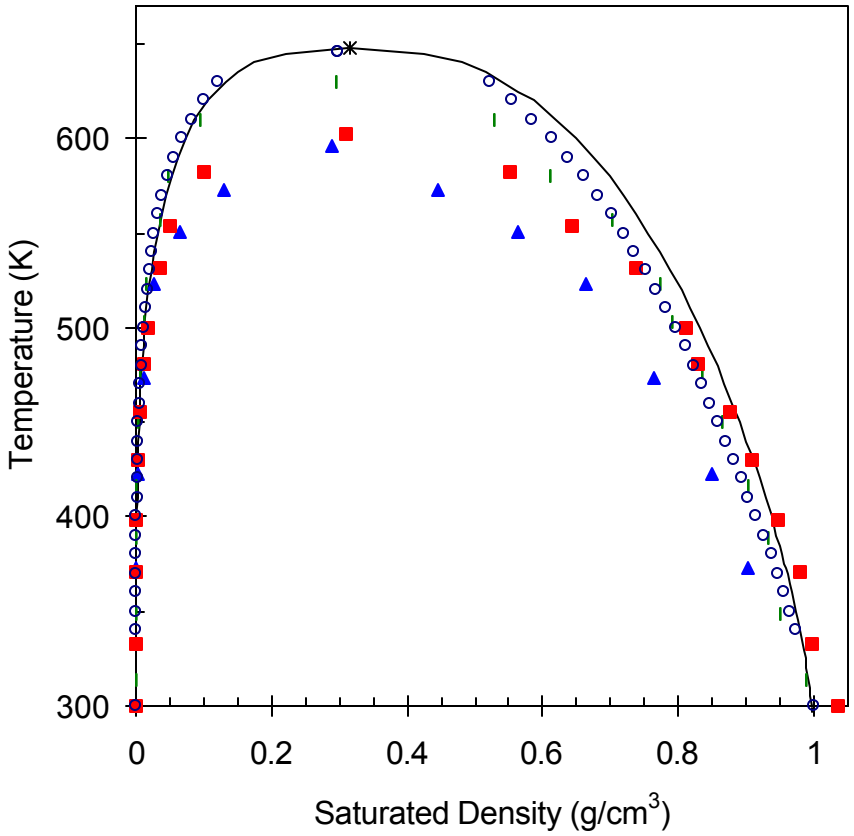
Temperature (K)
600
500
400
300
0
0.2
0.4
0.6
0.8
1
Saturated Density (g/cm3)

Figure 1

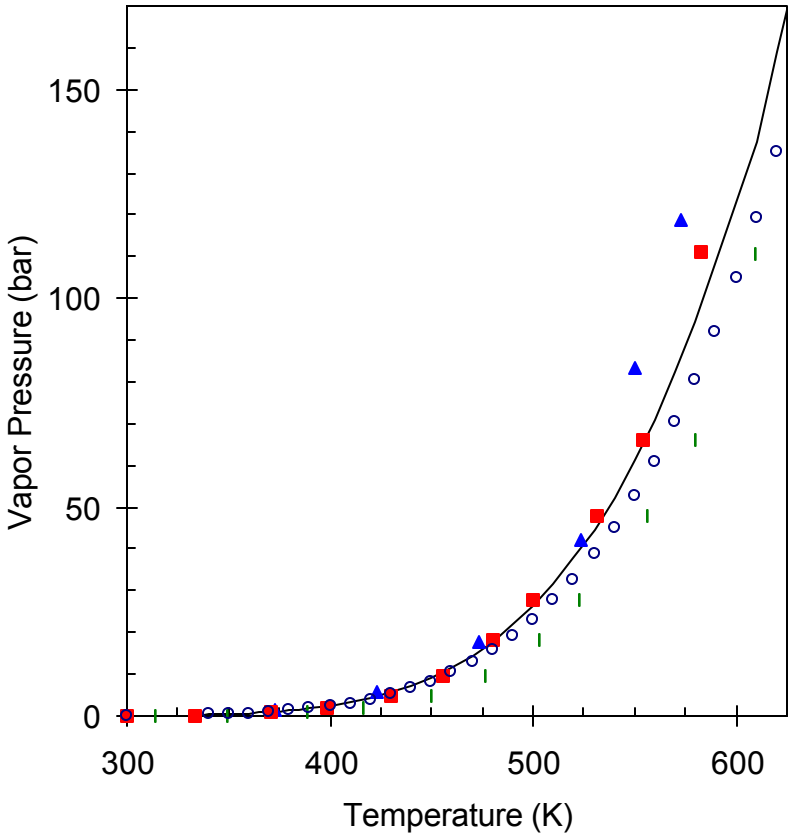

Figure 2

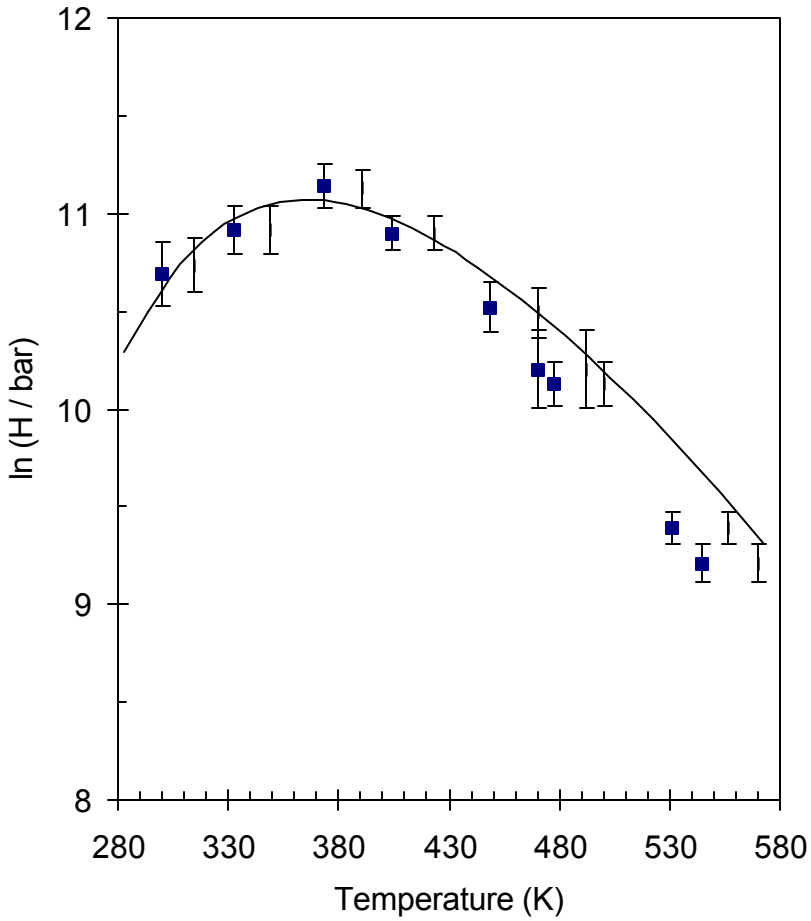

Figure 3

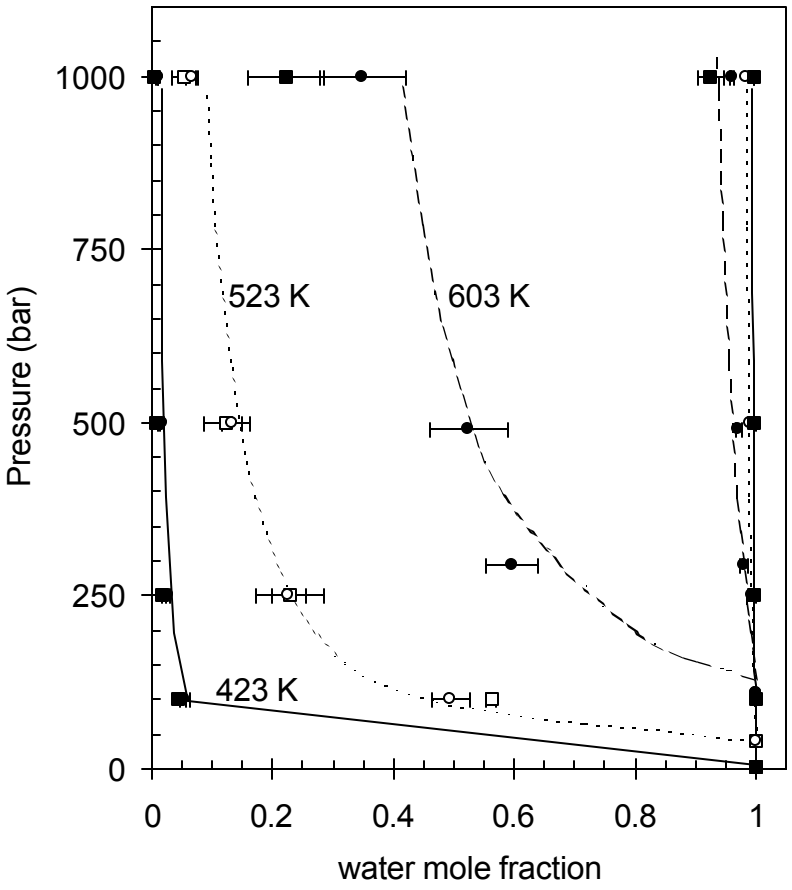
1000
750
500
250
0
Pressure (bar)
523 K
603 K
423 K
0
0.2
0.4
0.6
0.8
1
water mole fraction

Figure 4

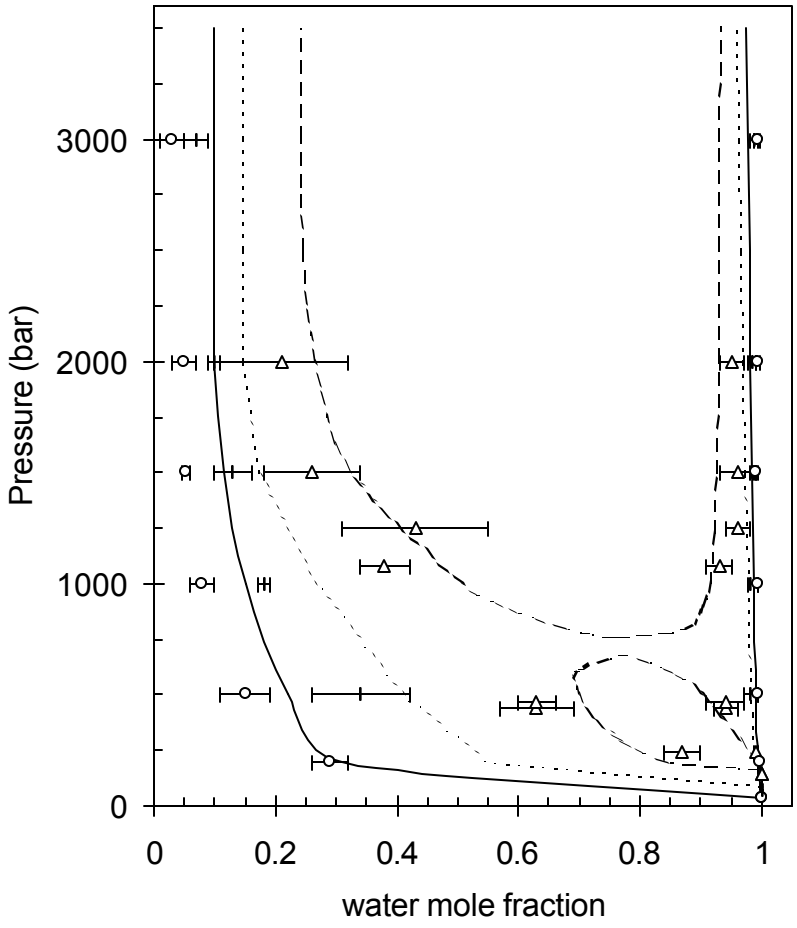
Pressure (bar)
3000
2000
1000
0
0
0.2
0.4
0.6
0.8
1
water mole fraction

Figure 5

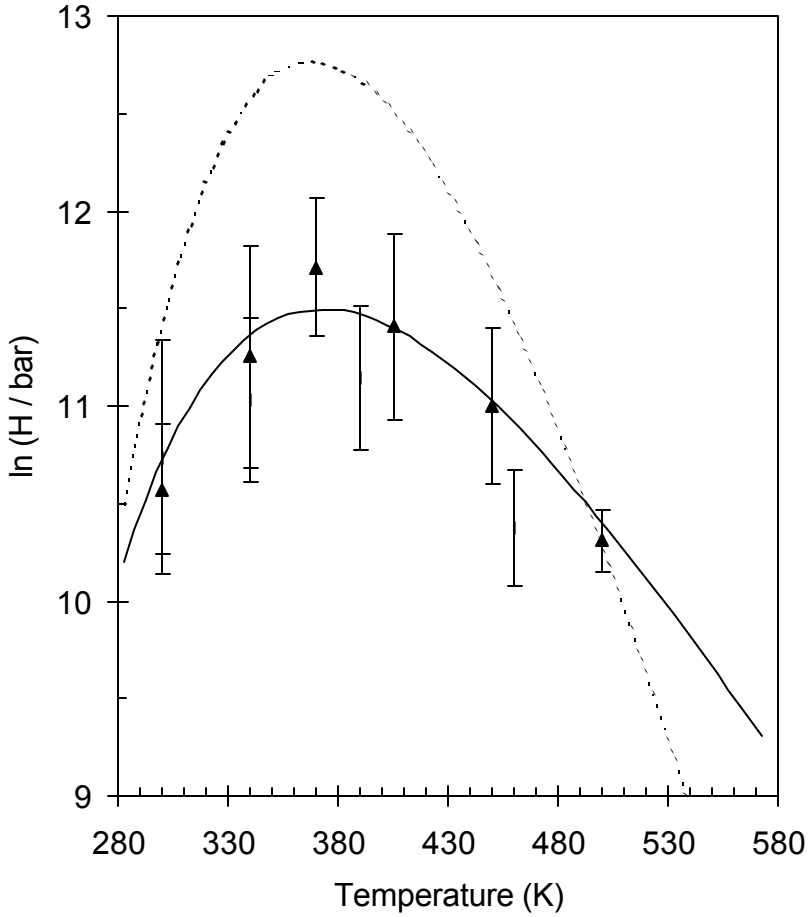

Figure 6

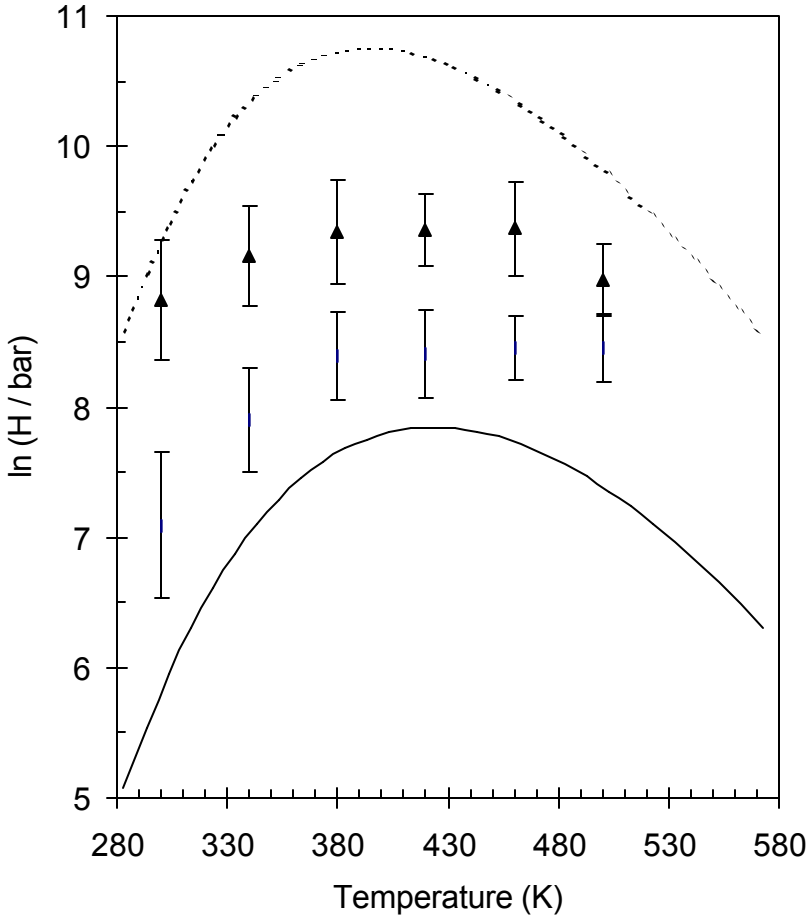

Figure 7